JOURNAL OF MATERIALS SCIENCE 26 (1991) 4545–4553

Advantage of the scanning tunnelling microscope in documenting changes in carbon fibre surface morphology brought about by various surface treatments

W. P. HOFFMAN, W. C. HURLEY, T. W. OWENS, H. T. PHAN
Air Force Astronautics Laboratory, AI/RKPB, Edwards, CA 93523, USA

The scanning tunnelling microscope (STM) was used to examine the surfaces of P-55 pitch-based carbon fibres before and after they had experienced various surface treatments (to $<1\%$ weight loss), which included treatment in an argon plasma, as well as oxidation in air at elevated temperature, oxygen plasma at room temperature, nitric acid bath, and an electrochemical bath. The effects of these surface treatments on the filaments could be differentiated from the micrometre scale down to the nanometre scale. The STM has been shown to be a valuable tool for viewing the surface morphology of these 10 μm filaments non-destructively in air down to the atomic scale.

1. Introduction

Carbon fibres are a very useful material in the fabrication of structural composites. Because of their high specific strength and modulus, composites made with carbon fibres are finding increased use especially in aerospace, astronautical and sporting goods applications. For a particular fibre–matrix system, the mechanical properties of these composites are determined to a great extent by the degree of bonding between the fibre and the matrix material which can be carbon, phenolic, epoxy, etc. Of course, other factors, such as fibre volume fraction, fibre orientation, and density also contribute to the mechanical properties of the finished composite.

The bond between the fibre and the matrix can have both a chemical component and a physical component. The chemical component is related to the number of chemical bonds between the matrix material and the accessible carbon active sites, which are sites where the valency is not satisfied. On a clean carbon surface, these active sites would be located on the edges of exposed layer planes as well as at imperfections in the structure including vacancies, dislocations, and steps in the outer basal plane [1]. In general, the physical component increases with the total surface area. This includes contributions from the surface roughness as well as the porosity, which affect the degree of mechanical interlocking. In a carbon–carbon composite the physical component may increase or decrease with surface roughness depending on the magnitude and geometry of the roughness and how this affects fibre wetting by the matrix material [2]. In this paper we have studied the effects of various surface treatments which will each affect both components of the fibre–matrix bond to varying degrees.

Fibre surface treatment methods have typically been empirically derived and thus little is known on the atomic scale about the chemical and structural changes that these procedures have produced. Obviously, being able to quantify the effects of various surface treatments is of great interest because this will aid in tailoring the mechanical properties of the composite. In the past it has only been possible to characterize the bulk or average changes that resulted from surface modification and from these bulk changes to infer changes in microscopic structure. However, with the invention in 1982 of the scanning tunnelling microscope (STM) [3] it has become possible to characterize the localized changes in surface morphology of carbon fibres down to the nanometre scale. A previous study [4] with the STM has shown that the carbon fibre surface can now be viewed non-destructively in air, vacuum, or under liquid on the atomic scale.

The scanning tunnelling microscope is a powerful tool that operates using the principle of quantum mechanical tunnelling between the metallic tip of the STM and a conducting surface [5, 6]. It is a useful instrument for characterizing the carbon fibre surface and modifications to the fibre surface because no sample preparation is required. For example, it is not necessary to coat or thin the sample or to observe it in vacuum, as is necessary with the scanning electron microscope (SEM) or the transmission electron microscope (TEM). Thus, the sample can be viewed non-destructively without disturbing the surface structure or adsorbed groups. One of the main drawbacks of the STM is the limited field of view at the atomic scale. Thus, it is difficult to determine what is characteristic of a particular surface because one can look at only

0022–2461/91 $03.00 + .12

one small area at a time. This problem can be overcome by looking at a large number of areas which, of course, is very time consuming. As is apparent, this problem is less severe on the micrometre scale.

For the global surface properties, the total fibre surface area can be measured by physical adsorption of krypton at 77 K using the BET equation [7], while the concentration of chemical bonding (active) sites per unit area can be determined by chemisorption of oxygen at 573 K [8], titration techniques [9, 10], and various spectroscopic techniques [11–14]. Of these three types of technique, the chemisorption of oxygen is considered the most useful and is the technique that is most often employed.

In this preliminary study, the surface of as-received P-55 carbon fibre without surface treatment, as well as the surface of P-55 samples treated commercially (electrolytically), and samples treated in our laboratory using nitric acid, oxygen and argon plasma, and oxidation in air, has been examined using the STM and gas adsorption techniques.

2. Experimental procedure

2.1. Treatments

The P-55 pitch-based carbon fibre used in this study was obtained unsized both with and without commercial surface treatment from Amoco Performance Products. The commercial surface treatment involves a proprietary process in which the fibre is passed through an electrolytic bath. In our laboratory, fibre samples without surface treatment were exposed to numerous processes. Fibres were oxidized in both 1 M nitric acid at 323 K and concentrated boiling nitric acid at 356 K for up to 24 h. A Branson/IPC S3000 Plasma system was used to treat fibre samples in both argon and oxygen. For these treatments a gas flow rate of 50–100 $cm^3\ min^{-1}$ and a power of 25–100 W were used. Other fibre samples were oxidized in flowing air at 773 K.

2.2. Instruments

Scanning electron micrographs were obtained on an ISI model CL6 scanning electron microscope. A Nanoscope II scanning tunnelling microscope (Digital Instruments, Santa Barbara, CA) was used to view the untreated surface morphology as well as the changes in surface morphology resulting from the various surface treatments from the micrometre to the fraction of a nanometre range. A 9 μm scan head was used to scan across the 10 μm fibre while a 0.6 μm head was used to observe atomic details in the constant current mode.

An STM functions on the basis of the quantum mechanical tunnelling of electrons under the influence of a small bias voltage ~ 25 nV in this study between an extremely sharp (ideally terminating in a single atom) metallic tip and a conducting surface separated by a gap of less than a nanometre. As the tip (Fig. 1) is moved in three dimensions with an x, y, z piezoelectric translator, it can trace the contours of the surface with atomic resolution. This extremely high resolution is

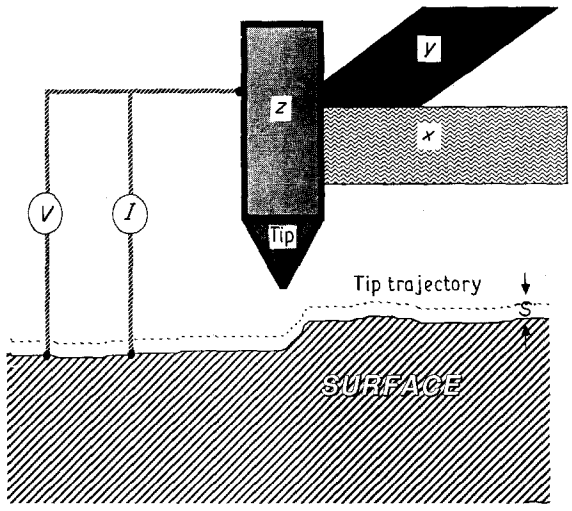

Figure 1 Schematic diagram of a scanning tunnelling microscope showing the essential elements which include a sharp metallic tip connected to a piezoelectric tube as well as the bias voltage and a means to measure the tunnelling current.

achievable because the tunnelling current is very sensitive to the distance between the tip and the surface. The current 2–9 nA in this study typically will change by a factor of at least 2 for a change in distance of 0.1 nm.

In the constant current mode used in this study, the tip is rastered across the surface while the tunnelling current (2–9 nA) is kept constant by a feedback control circuit. In this mode, voltage is applied to the z-piezoelectric translator to raise and lower the tip in order to keep the tunnelling current constant. This variation in voltage is used along with the x–y raster voltage to generate the three-dimensional image of the surface.

2.3. Surface-area measurements

The total surface area of the fibre samples was measured on a Micromeritics Digisorb 2500 automated adsorption instrument. Krypton, which was assumed to be in the solid form with a cross-sectional area of 0.214 nm^2/atom [15], was used as the adsorbent at 77 K.

To determine the concentration of active sites on the fibre, oxygen was chemisorbed at 573 K and 67 Pa using the technique first developed by Laine *et al.* [16] and later modified for carbon fibres [17, 18]. The procedure starts with cleaning a carbon sample at 1223 K in high vacuum (10^{-6} Pa). After the sample is cleaned, it is cooled to 573 K and oxygen is dissociatively chemisorbed for 16 h. At the end of this time, the sample is evacuated to a pressure of 10^{-6} Pa with the temperature held at 573 K. Pumping is then terminated and the temperature is raised to 1223 K (30 K min^{-1}) and held at that temperature for 20 min. Because the surface area of the carbon fibres is so small, each sample was cooled to 573 K and a second desorption cycle was run as a blank. During each cycle, the amount of CO and CO_2 that desorbs is measured. Knowing the number of moles of each gas desorbed by the sample, and taking the area of an active carbon site that chemisorbed an oxygen atom

as 0.083 nm^2, the surface area occupied by oxygen (active surface area) can be determined.

3. Results and discussion

3.1. As-received P-55 fibre

Carbon fibres have been surface-treated for many years in order to improve the adhesion between the fibre and the matrix material. Using the scanning tunnelling microscope (STM) it is now possible to see the effects of the commercial treatment as well as other mild surface treatments, which involve minimal fibre weight loss. It is important to minimize weight loss during surface activation to maintain the excellent mechanical properties of the fibre. In this preliminary study, the samples were activated to a greater extent than is done in the present commercial process or would be done in any new future process. The reason for this degree of activation was to be sure that there was enough change in the surface to be observed. Obviously, the mechanical properties of these samples were degraded to some extent.

A scanning electron micrograph that has not been surface treated is shown in Fig. 2. At this magnification (mag $\times 3.3 \times 10^3$), the relatively smooth surface of the 10 μm fibres is clearly visible. Also, one can see the axial striation marks from the extrusion process and the carbon "dirt" stuck to the surface that also originated during the manufacturing process. When we attempted to use our SEM to observe the surface of this fibre that had undergone mild surface treatment, we met with limited success. Even at higher magnification, it was not possible to view significant differences in the fibre surface morphology after some of the surface treatments.

With the STM, however, it was possible to differentiate the small changes in the fibre surface that resulted from our various mild surface treatments. (Some of these changes were not even detected by our gas adsorption techniques.) In Fig. 3 one can see the surface of an untreated P-55 pitch-based carbon fibre viewed at a slightly higher magnification using the STM. The striation marks parallel to the fibre axis are still visible. The micrograph shows clearly that although the surface is not flat, the contours on this fibre are smooth. This is also the case at higher magnification (Fig. 4) and is in contrast to other fibres such as a PAN fibre, for instance, where the surface contours are not smooth, resulting in sharp steps on the surface [19]. On the atomic scale, there are some small graphitic regions on the P-55 surface (Fig. 5), but the majority of the surface consists of amorphous and various nongraphitic structures such as seen in Figs. 6 and 7. Because of the increase in surface roughness, it was not possible at this time to obtain micrographs on the atomic scale on the majority of the samples exposed to the various surface modifications.

3.2. Fibre exposed to air at 823 K

Fig. 8 is a 6.0 μm scan of a P-55 fibre exposed to air at 823 K which resulted in 0.76% weight loss. It can be

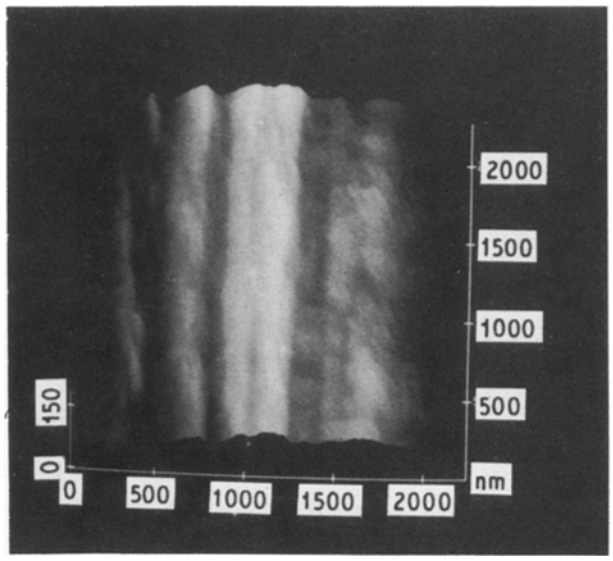

Figure 3 Scanning tunnelling micrograph of a P-55 carbon fibre surface showing axial striations and some dirt in this 3-D image that measures 2 μm in both x and y.

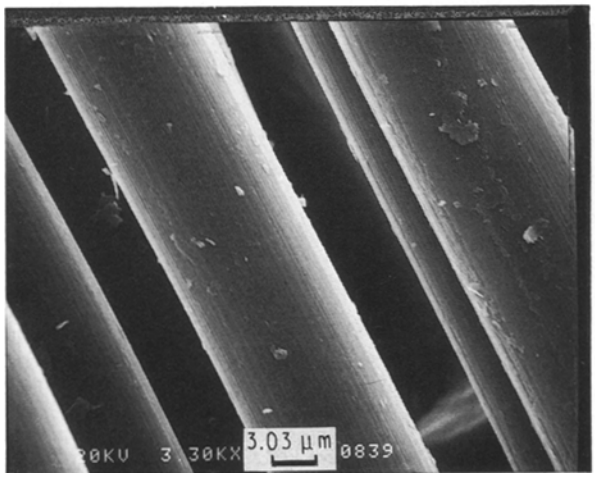

Figure 2 Scanning electron micrograph of the surface of a P-55 carbon fibre showing axial striations and some dirt from the manufacturing process on these 10 μm fibres.

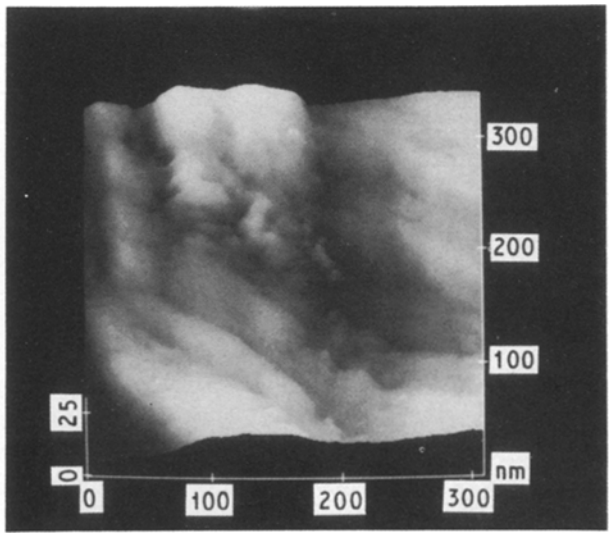

Figure 4 Smooth contours on surface of P-55 fibre as seen at higher magnification by the STM in this 300 nm × 300 nm grey scale top view.

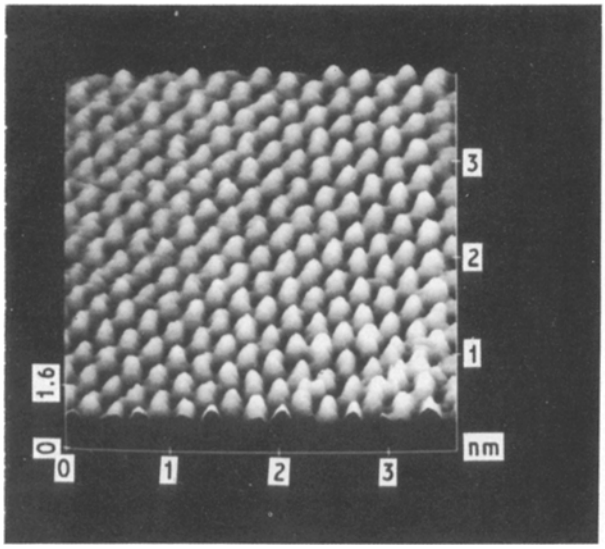

Figure 5 Small graphitic region on the carbon fibre surface can be seen in this 3.5 nm × 3.5 nm grey scale image.

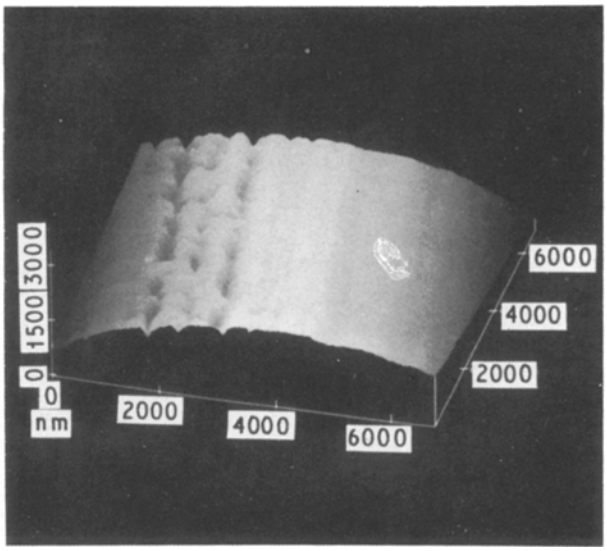

Figure 8 Localized pitting of carbon fibre surface resulting from oxidation in air at 823 K to 0.76% weight loss. The curvature of the fibre can be seen in this 6.5 μm scan.

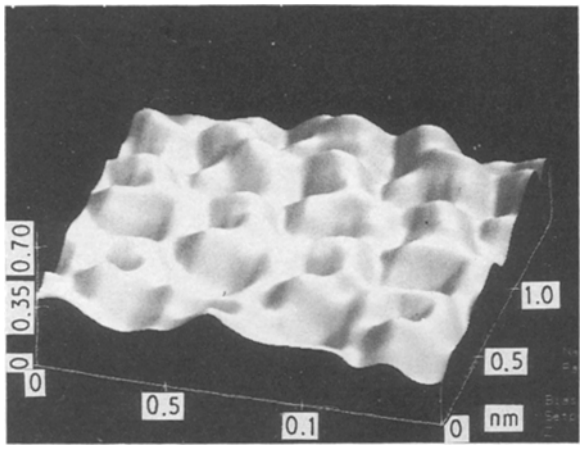

Figure 6 One of the many disordered structures on the surface of the P-55 fibre. It appears as though one atom in the ring is missing in this 3-D image that spans 1.5 nm in both x and y.

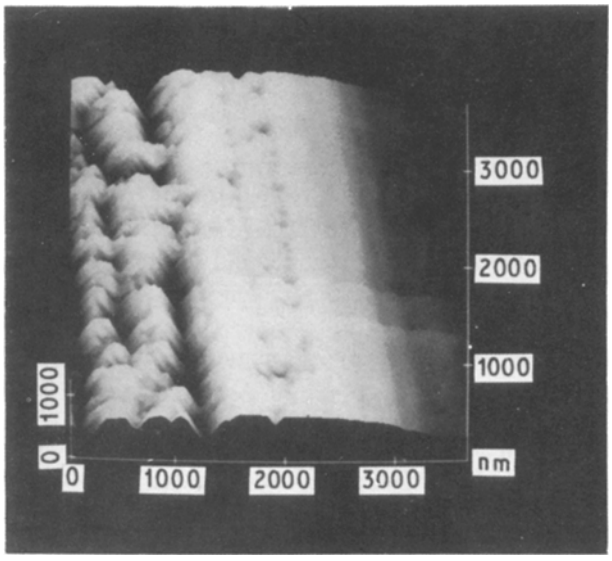

Figure 9 Higher magnification view of the pitting in Fig. 8. Note extent of pitting and the fact that the pits are relatively shallow in this 3.5 μm × 3.5 μm grey scale top view.

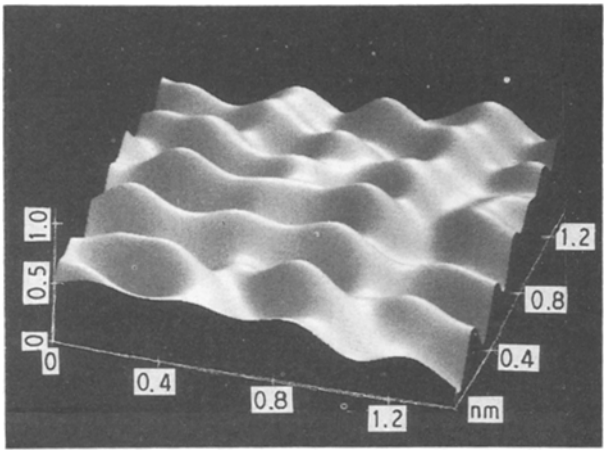

Figure 7 This 3-D image that measures 1.4 nm in both x and y shows another disordered structure seen on P-55 fibre.

seen that this treatment caused pitting that is not uniform across the surface but is localized in a band that runs parallel to the fibre axis. Because oxidation in air occurs at carbon-active sites [16], it is assumed that this preferential oxidation is taking place in a more disordered region that was formed in the manufacturing process. In an enlarged view of this region (Fig. 9) the details of the pitting are more clearly seen. There is obviously a distribution in the diameter of these pits which are about three times as deep as they are wide. Although the majority of the pits are localized in a band, there are much smaller pits located in the regions that appear smooth in Figs. 8 and 9. One of these pits with a diameter of about 70 nm is shown in Fig. 10. This pitting increased both the total as well as the active surface area of the fibres as seen in Table I.

3.3. Oxygen plasma treatment at room temperature

In contrast to the micrographs obtained on samples exposed to air at high temperature, the images obtained on samples treated in an oxygen plasma at

TABLE I

Treatment	Weight loss (%)	ASA ($m^2 g^{-1}$)	BET ($m^2 g^{-1}$)
No treatment	0	0.034	0.46
Air oxidation	0.76	0.097	0.521
Oxygen plasma	0.66	0.077	0.501
	6.21	0.097	0.559
Argon plasma	0.66	0.070	0.334
Commercial	[a]	0.029	0.44
Concentrated HNO_3	1.4	0.23	1.21
1 M HNO_3	[b]	0.027	0.513

[a] Not known.
[b] Too small to detect.

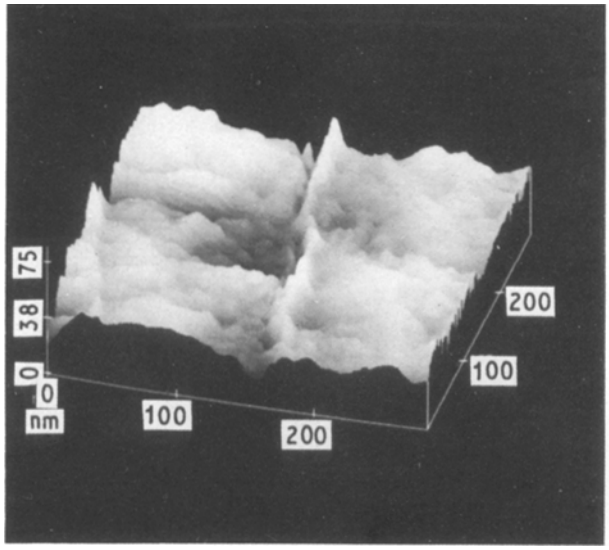

Figure 10 A 300 nm × 300 nm enlargement of the centre of Fig. 9 shows a small pit in an region in which no pitting was observed at lower magnification.

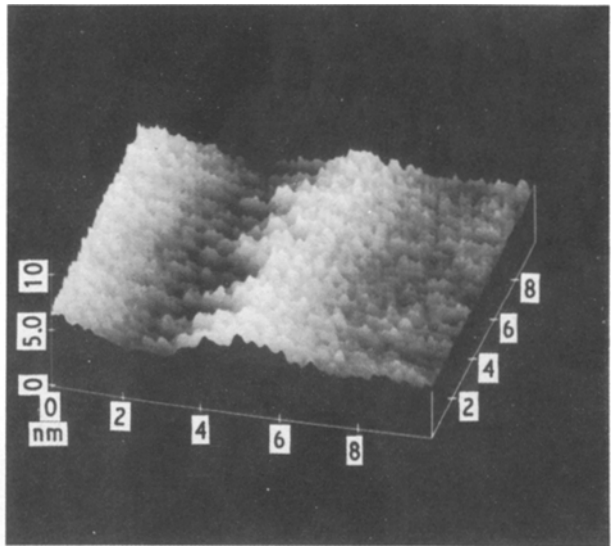

Figure 11 Fibre surface treated in atomic oxygen to 0.66% weight loss shows fairly uniform etching of the surface in this 3-D image that measures 9 nm in both x and y.

room temperature are a little more difficult to explain. Because atomic oxygen at room temperature is able to remove carbon atoms from a perfect basal plane region as well as from discontinuities in the structure [20, 21], one would expect that the surface of a carbon fibre treated in atomic oxygen would not be appreciably pitted. This was the case on the atomic scale at low burn-offs (Fig. 11) but not at lower magnification or with higher activation. It can be seen from the scanning tunnelling micrographs of a P-55 fibre treated in an oxygen plasma to 0.66% weight loss that, although the surface on the atomic scale (9 nm scan) seems uniformly roughened (Fig. 11), at lower magnification (Fig. 12) fairly deep pits (40–125 nm) are uniformly spread over the surface. This has been observed by others at lower magnification [22].

There was no visible effect of oxidation with oxygen plasma on the micrometre scale at this low burn-off as there was with molecular oxygen with $< 1\%$ weight loss. Because of this, another sample was oxidized in the oxygen plasma to 6.21% weight loss to see the results of a more extensive oxidation. In Fig. 13, which is a 3 μm scan across this fibre sample, pits can be seen fairly uniformly distributed across the surface. The details of a 100 nm diameter pit can be seen in Fig. 14.

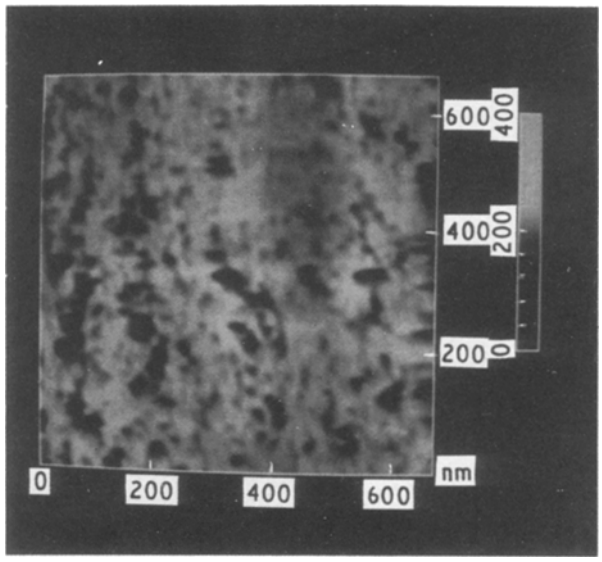

Figure 12 Relatively deep pits that are uniformly distributed over this 700 nm × 700 nm area are observed at lower magnification on the same sample as in Fig. 11.

These pits formed by atomic oxygen differ from those formed in air not only by their distribution on the surface but also by their aspect ratio. The pits formed by atomic oxygen at this level of activation are 15

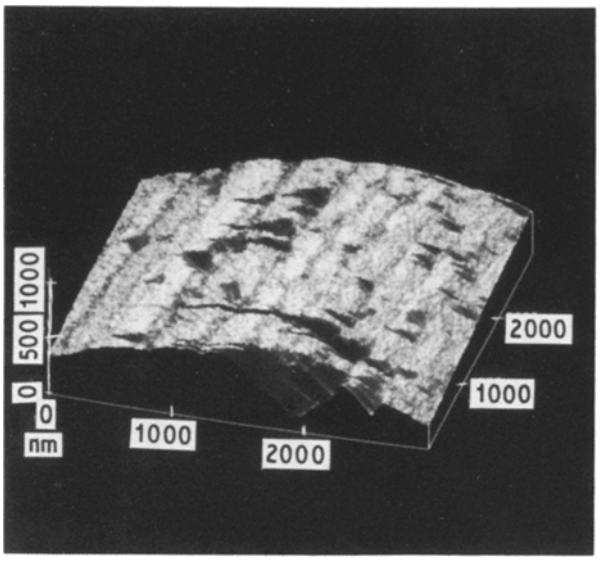

Figure 13 Rather uniform pitting is visible on this fibre surface treated in atomic oxygen to 6.21% weight loss. The curvature of the fibre can be seen in this 3-D image that measures 3 μm in both x and y.

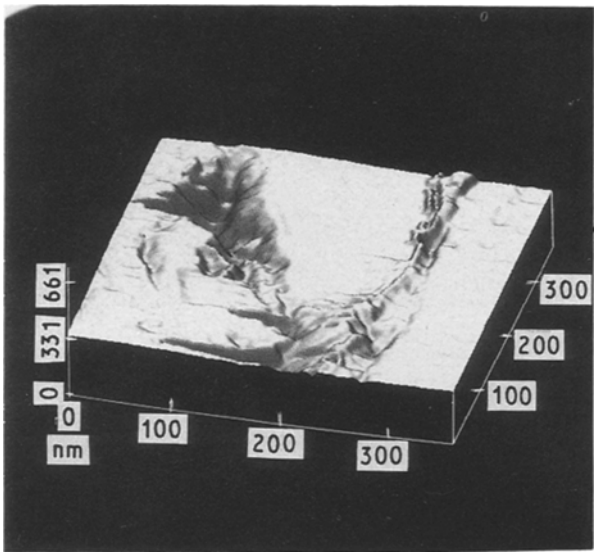

Figure 14 A 350 nm scan of a rather deep pit seen in Fig. 13. Note that the pit is approximately 15 times as deep as it is wide.

times as deep as they are wide and appear similar to what one would expect in a catalysed reaction. (Although different tips were used and thus an exact comparison of the aspect ratio of the pits formed by molecular and atomic oxygen cannot be made, at these magnifications it can be stated that the aspect ratio of oxygen plasma pits is greater than for those pits formed in air.)

Thus, at low levels of activation on the atomic scale, the surface is rather uniformly roughened but after additional weight loss the atomic oxygen attack has formed rather deep pits that are rather evenly distributed across the surface. Others have also seen irregular etch pits on the basal plane [22] like those seen in Fig. 12 and have observed that less-ordered carbon and edge sites will oxidize faster in atomic oxygen [23–24]. Thus, although atomic oxygen is more reactive than molecular oxygen and is able to remove basal plane atoms at this temperature, the structural heterogeneity in the carbon fibre still gives rise to preferential etching. The pitting of both fibre samples exposed to oxygen plasma was reflected in an increase in both the active and total surface areas of these fibres (Table I).

3.4. Argon plasma treatment

Using an inert gas plasma such as argon at room temperature to activate the surface by atomic bombardment does not increase the total surface area of the fibre even with 0.66% weight loss although it does increase the active surface area as measured by oxygen chemisorption (Table I). This is difficult to explain on the basis of the information that was obtained from the scanning tunnelling micrographs, especially on the micrometre scale. Fig. 15 is a micrograph on the atomic scale of a fibre surface exposed to an argon plasma until 0.66% of the fibre weight was removed. The micrograph presents what looks to be a nearly graphitic region with a closest-neighbour distance of 0.142 nm where some of the atoms are missing. This is what might be expected from the inelastic collisions of energetic argon atoms with the surface which results in

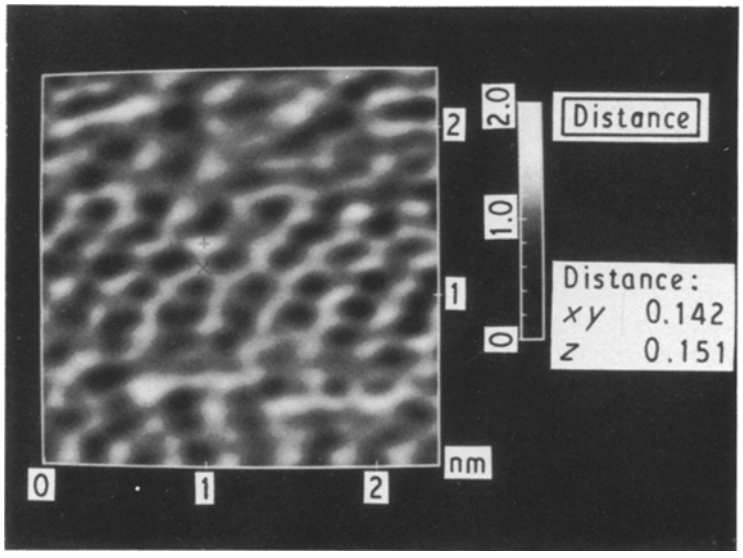

Figure 15 Atomic structure of a carbon fibre surface after exposure to an argon plasma that resulted in 0.66% weight loss. Missing atoms are evident in this 5 nm × 5 nm grey scale top view image.

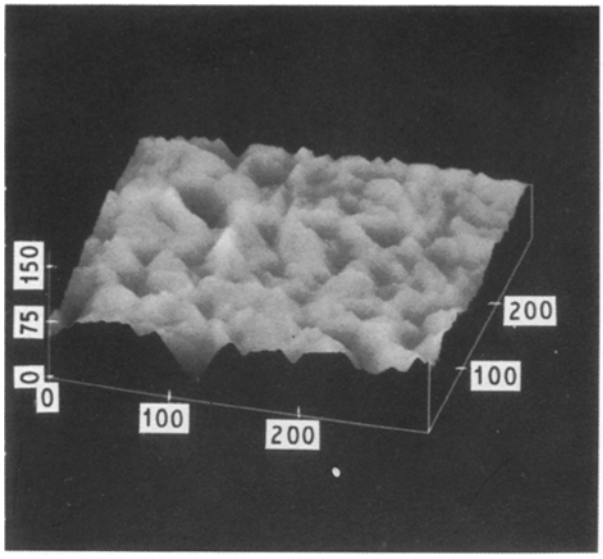

Figure 16 A lower magnification view of the same sample as in Fig. 15 detailing the surface roughness brought about by argon plasma treatment (300 nm scan).

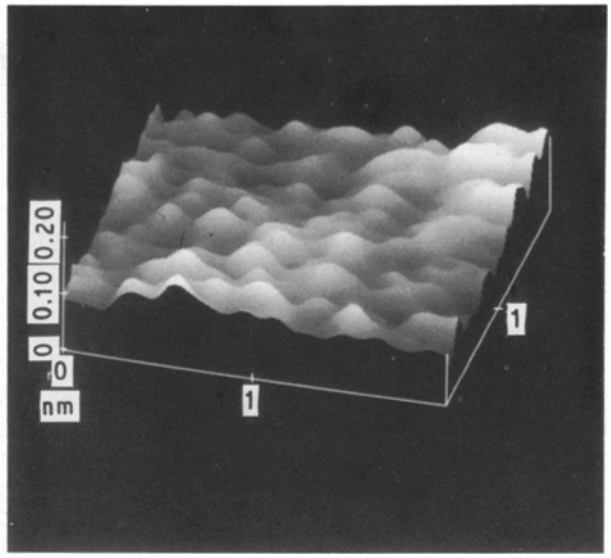

Figure 17 Atomic image of a P-55 fibre after being exposed to the commercial surface treatment. 3-D image spans 2 nm in both x and y.

the erosion of the surface one atom at a time. We did not see this structure on other surfaces but cannot definitively say that it was not part of the untreated surface because the number of as-received samples that we studied was relatively small.

The micrographs presented thus far have shown that the STM has given us the opportunity to view the surfaces of carbon fibres nondestructively at magnifications never before possible. This is, of course, a two-edged sword. We are able to answer some questions that we were not able to answer before, but, on the other hand, what we are able to observe at these higher magnifications also generates other questions for which we do not have answers at this time. One of the questions that quite possibly has been answered has to do with the commercial surface treatment and nitric acid treatment described below.

On the other hand, scanning tunnelling micrographs of carbon fibres exposed to argon plasma treatments have generated new questions. It was mentioned above that the deep pitting observed with extensive oxidation in oxygen plasma is not well understood. There is a similar situation with fibres treated in argon plasma. At a magnification of 1.7 $\times 10^5$ (Fig. 16) pits of less than 35 nm deep can be seen distributed across the surface. We think that these pits, as well as those seen at lower magnification, result from a variability in the hardness in the surface. However, the origin of these pits is not as much of a question as why this amount of pitting and surface roughening actually decreases the total surface area (Table I) rather than increasing it. One possible explanation is that the argon bombardment is only removing a loose surface layer revealing a more active higher density surface of lower total area.

3.5. Commercial treatment

The commercial surface treatment, which consists of etching in an electrochemical bath [25], does not

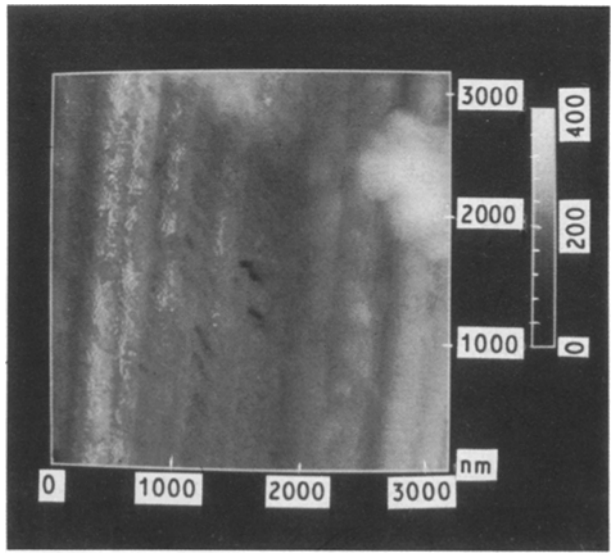

Figure 18 P-55 fibre after exposure to commercial surface treatment. Axial striations and dirt as well as pitting are evident in this 3 μm × 3 μm top view.

significantly increase the total surface area of the fibre, and in addition it actually decreases the active surface as measured by oxygen chemisorption (Table I). However, in spite of these facts the process does increase the degree of fibre–matrix bonding. This is quite possibly due to the removal of surface defects from the fibre surface. On the atomic scale in the regions in which we looked, the surface did not look appreciably different (Fig. 17) than the untreated surface. On the micrometre scale (Fig. 18) the surface had some small pits localized in bands running parallel to the fibre axis. This is similar to what was observed for the fibre oxidized in air. It is quite possible that the currently held model [26] is correct, i.e. that the commercial surface treatment increases fibre–matrix bonding by simply removing a loose surface layer that does not contribute to bonding. Although we did not see evidence for this in our limited study on the commercially surface-treated fibre, we did see evidence for this

phenomenon when the fibre was treated in mild nitric acid as described below. Clearly, on the commercially treated fibre as well as on these other treated fibre surfaces, much more in-depth work needs to be done.

3.6. Exposure to 1 M HNO_3 at 323 K

When P-55 fibres were exposed to a mild (1 M) nitric acid treatment for 24 hr at 323 K, some interesting results similar to those for argon etching were obtained. On these samples there was no significant increase in the total surface area and there was actually a small decrease in the active surface area as measured by oxygen chemisorption (Table I). In addition, with the SEM we were not able to see significant changes in the surface on the micrometre scale. This is similar to what we saw on the commercially surface-treated fibre. In Fig. 19 the axial striations run from the lower left to the upper right of the micrograph. At first glance at this magnification, the surface appears identical to an untreated fibre. However, a closer look reveals small lines running parallel to the fibre axis. At higher magnification (Fig. 20) these lines are actually cliffs which have a great deal of detail. Because neither the active nor the total surface area increase with this mild treatment, it is possible, that these cliffs appear after the removal of some loosely bound material from the surface. This has been assumed in the past to account for the enhanced adhesion that results from the commercial surface treatment.

3.7. Concentrated nitric acid treatment at 356 K

In contrast to the mild nitric acid treatment, boiling (356 K) concentrated nitric acid has a very pronounced effect on the fibre surface morphology as well as on the total and active surface area. At 1.5% weight loss, boiling nitric acid enhanced both the total and active surface area to a greater degree than the other techniques achieved (Table I). However, this treatment

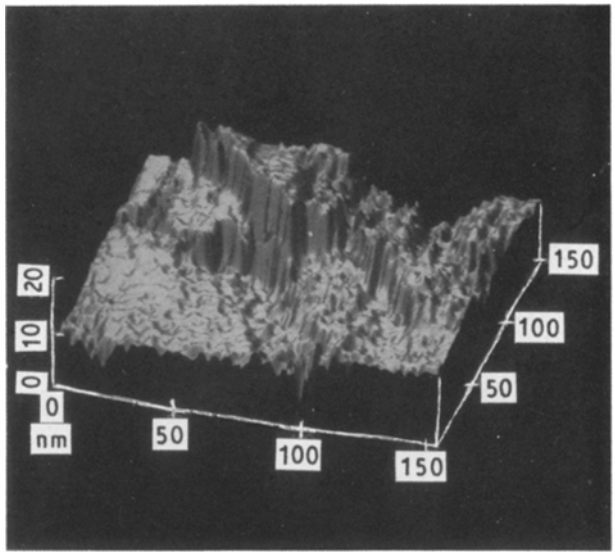

Figure 20 A 150 nm × 150 nm blow-up of one of the lines seen on the surface in Fig. 19 reveals that it is actually a cliff with a great deal of detail.

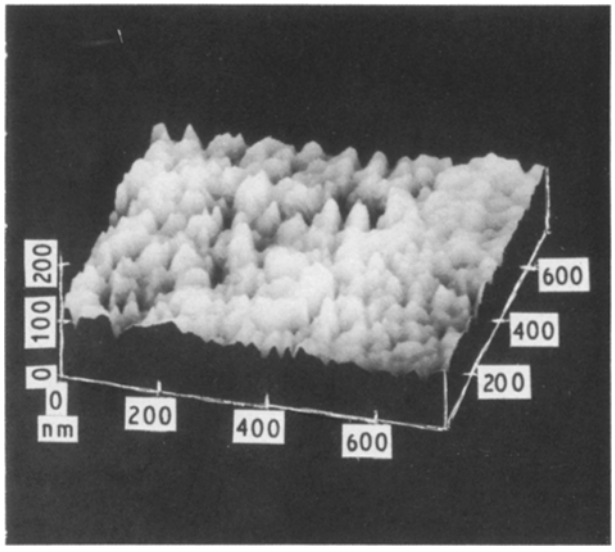

Figure 21 The roughening of the surface after exposure to concentrated HNO_3 at 356 K for 24 h is evident in this 700 nm × 700 nm 3-D image.

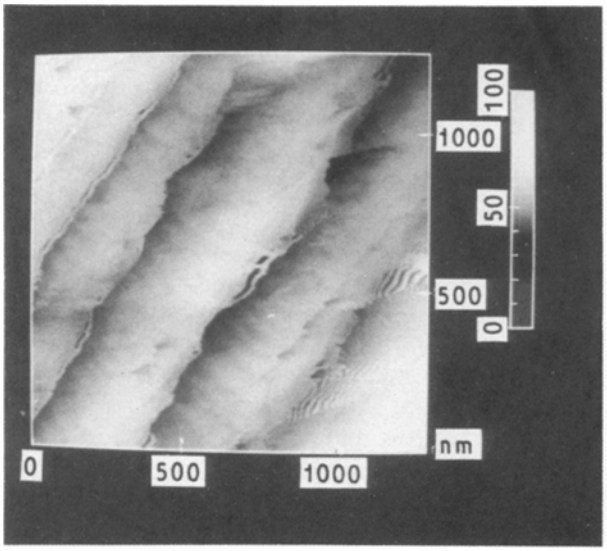

Figure 19 This 1.2 μm × 1.2 μm grey scale top view image demonstrates that small axial lines are evident in the surface after exposure to 1 M HNO_3 for 24 h at 323 K.

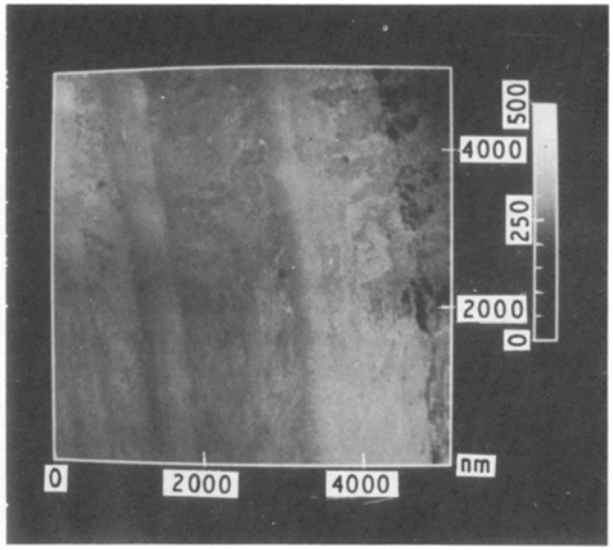

Figure 22 Even at lower magnification, the surface roughening due to treatment in concentrated HNO_3 at 356 K for 24 h is apparent in this 5 μm scan.

is not recommended, because it seriously degraded the integrity of the fibre. The micrographs of this fibre illustrate that the above changes are caused by a significant roughening of the surface. At a magnification of 70×10^3 (Fig. 21), the treated surface is covered with shallow holes of 30 nm that are uniform in size and distribution across the surface. Even at lower magnification (Fig. 22) the surface appears very rough.

4. Conclusion

This survey of the effect of various surface treatments for carbon fibre surfaces was not meant to give a definitive description of each fibre surface but rather to show the usefulness of the STM in being able to discern differences in the surfaces of mildly treated fibres. The surfaces were treated to a greater extent than would be feasible commercially in order to be certain that differences could be observed. Obviously, there is much further work needed to statistically describe the surface of each of these treated fibres. In addition, the micrographs presented in this communication have generated questions that cannot be answered without further study. However, these micrographs do demonstrate that the STM is a unique tool that will be extremely useful in the study of adhesion of carbon fibres in various matrix materials.

Acknowledgement

The financial support of the Air Force Office of Scientific Research is greatly appreciated.

References

1. W. P. HOFFMAN, F. J. VASTOLA and P. L. WALKER Jr, *Carbon* **22** (1984) 585.
2. F. R. EIRICH, in "Interface Conversion for Polymer Coatings" (Elsevier, New York, 1968).
3. G. BINNIG, H. ROHRER, Ch. GERBER and E. WEIBEL, *Phys. Rev. Lett.* **49** (1982) 57.
4. W. P. HOFFMAN, V. B. ELINGS and J. A. GURLEY, *Carbon* **26** (1988) 754.
5. C. F. QUATE, *Physics Today* August (1986) 26.
6. P. K. HANSMA and J. TERSOFF, *J. Appl. Phys.* **61** (2) (1987) R1.
7. S. BRUNAUER, P. H. EMMETT and E. J. TELLER, *Amer. Chem. Soc.*, **60** (1938) 309.
8. W. P. HOFFMAN, F. J. VASTOLA and P L. WALKER Jr, *Carbon* **26** (1988) 485.
9. H. P. BOEHM and E. DIEHL, *Angew. Chem. Int. Edn.* **3** (1964) 10.
10. B. CHUN and R. R. GUSTAFSON, in Extended Abstracts, 19th Conference on Carbon, Pennsylvania State, June 1989, p. 78.
11. C. KOZLOWSKI and P. M. SHERWOOD, *Carbon* **25** (1987) 751.
12. A ISHITANI, in "Molecular Characterization of Composite Interfaces" (Plenum Press, NY, 1986) p. 321.
13. T. A. De VILBISS and J. P. WRIGHTMAN, in "Composite Interfaces", (North Holland, NY, 1986) p. 307.
14. J. ZAWADZKI, in "Chemistry and Physics of Carbon', Vol. 21 (Marcel Dekker, New York, 1989) p. 147.
15. I. M. K. ISMAIL, *Carbon* **28** (1990) 423.
16. N. R. LAINE, F. J. VASTOLA and P. L. WALKER Jr, *J Phys. Chem.* **67** (1963) 2030.
17. W. P. HOFFMAN and J. A. LOWRY, in Extended Abstracts, 16th Biennial Conference on Carbon, San Diego, June 1983, p. 357.
18. I. M. K. ISMAIL, *Carbon* **25** (1987) 653.
19. W. P. HOFFMAN, W. C. HURLEY, P. M. LIU and T. W. OWENS, *J. Mater Res.*, in press.
20. G. J. DIENES, G.R. HENNIG and W. KOSHIBA, in "Proceedings of the Society, International Conference on Peaceful Uses of Atomic Energy", Geneva, June 1958, Paper 1778.
21. N. M. RODRIGUEZ, S. G. OH, W. B. DOWNS, P. PATTABIRAMAN and R. T. K. BAKER, in Extended Abstracts, 19th Biennial Conference on Carbon, Pennsylvania State, June 1989, p. 564.
22. J. M. THOMAS, in "Chemistry and Physics of Carbon", Vol. 1 (Marcel Dekker, New York, 1965) p. 121.
23. H. MARSH, M. FORREST and L. PACHEO, *Fuel* **60** (1981) 423.
24. C. WONG and R. T. YANG *J. Chem Phys.* **78** (1983) 3325.
25. J. HARVEY, C. KOZLOWSKI and P. M. A. SHERWOOD, *J. Mater. Sci.* **22** (1987) 1585.
26. L. T. DRZAL, M. J. RICH and P. F. LLOYD, *J. Adhesion* **16** (1982) 1.

Received 18 July 1990
and accepted 24 January 1991